ELSEVIER

PII: S0032-3861(96)00707-0

Polymer Vol. 38 No. 8, pp. 1817–1833, 1997

0032-3861/97/$17.00 + 0.00

A temperature window of reduced flow resistance in polyethylene with implications for melt flow rheology: 3. Implications for flow instabilities and extrudate distortion

J. W. H. Kolnaar*† and A. Keller
H. H. Wills Physics Laboratory, Tyndall Avenue, Bristol BS8 1TL, UK
(Received 25 January 1996; revised 25 June 1996)

As a third and final part of this study on the temperature window of reduced flow resistance in polyethylene the consequences for flow instabilities and extrudate distortions have been investigated. Through the fact that, within the temperature window, melt extrusion could be carried out to much higher flow rates than usual without flow instabilities and extrudate distortions, we not only extended the practically useful throughput range, but also acquired a useful handle for the appreciation of such instabilities in general and for their control under more wide ranging conditions. Categorizing extrudate distortions as surface roughness, periodic bulk distortions and gross shape distortions, definitive confirmation was obtained that the site of gross shape distortions is at the entry orifice, that of periodic bulk distortions is in the capillary interior and those manifest as surface effects at the capillary exit. The latter two are absent under window conditions, but gross shape distortions (closest to what is conventionally referred to as 'melt fracture') always set in, i.e. both at window conditions and otherwise, when a critical stress level is attained. The corresponding critical flow rate was found to scale as a −1.5 power of the molecular weight. This combined with the previously found −4.0 power dependence of the critical flow rate for the window effect (at the appropriate temperature) serves to define the existence regime of the window effect in terms of flow rate and molecular weight. Effects investigated in some detail include the nature and the origin of pressure oscillations and also the effect of external lubricants. The influence of the latter is the creation of conditions similar to the window effect which, from this point of view, could be considered as corresponding to 'self lubrication'. Finally, the findings in the present work invite a general approach to flow instabilities and extrudate distortions on the basis of a specific stress criticality pertaining to each class of effects the underlying causes of which the present work has helped to identify.

(Keywords: surface roughness; periodic bulk distortions; gross shape distortions)

INTRODUCTION

This is the final part of a series of three papers on a recently discovered melt flow singularity taking place in the course of capillary extrusion of linear high molecular weight (M) polyethylene (PE) at around 150°C. As opposed to what is commonly observed for these high M melts at conventional processing temperatures (i.e. $T > 160$°C), within this 'window' the extruded filament is smooth and glossy and extrusion is accompanied by significantly reduced pressures, hence flow resistance.

As described in previous publications[1–6] the basic effect is depicted by *Figure 1* showing the extrusion pressure (p) recorded as a function of continuously increasing temperature (T) at constant piston velocity (v). For appropriately high M, and for a sufficiently high v there is a pronounced decrease in p within a narrow T range of 148–152°C (the temperature 'window') with a sharply defined minimum at 150–151°C.

The variables affecting this minimum are described in parts 1 and 2 of the series[5,6]. In line with previous works from this laboratory[1–4] the origin of the window effect is attributed to a phase transformation at the particular temperature. The formation of a transient, hexagonal crystal phase, which is known to contain the chains in a highly mobile form, was suggested, as created through flow-induced chain extension. Using a purposefully constructed rheometer, in a different study we could indeed identify this hexagonal phase within the capillary portion of the die by conducting high intensity *in situ* X-ray studies in the course of flow[7].

In part 2 it was shown that the site responsible for the window effect resides along the walls of the capillary[6]. This is in contrast to the previously held view[1–4] that the window effect originates in the elongational flow upstream of the capillary, which is known to induce the crystallization effects as first observed by van der Vegt and Smit[8]. In addition, the separation of effects in the entry orifice from those in the capillary pursued in part 2 provided an unexpected, new approach to the exploration of flow instabilities to be taken up further in

* Permanent address: DSM Research BV, PO Box 18, 6160 MD Geleen, The Netherlands
† To whom correspondence should be addressed

the present part. To this end, first the complex subject area of flow instabilities and extrudate distortions will be briefly introduced.

Flow instabilities and extrudate distortions

Since the pioneering studies by Nason[9], Tordella[10–13] and others[14–24] it has been known that, beyond a critical throughput, irregularities occur during melt extrusion. These irregularities, which are commonly referred to collectively as 'melt fracture', fall into two categories, namely instabilities during melt flow and extrudate distortions, and have not always been clearly delineated.

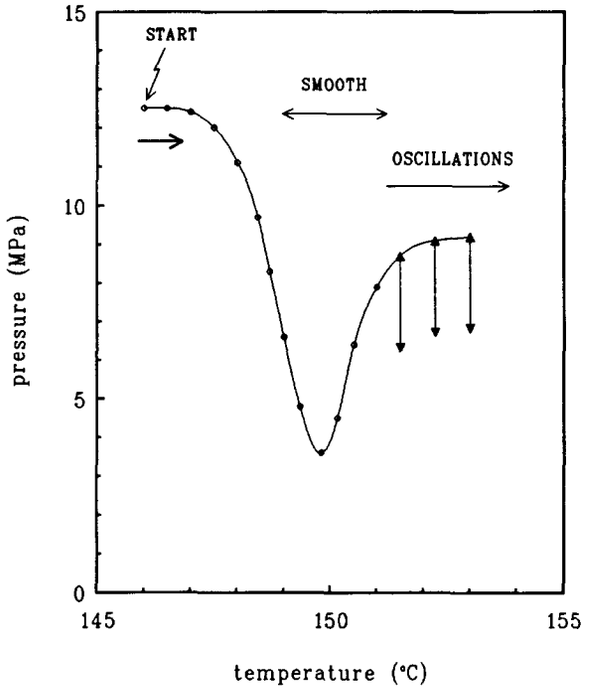

Figure 1 Pressure vs temperature trace showing the window effect[5]

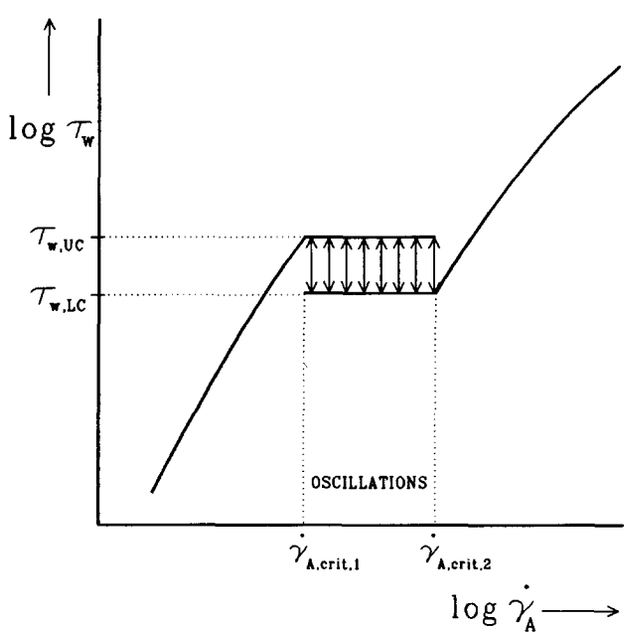

Figure 2 Schematic representation of the multi-valued flow curve for HDPE in case a fixed rate of extrusion is maintained. The vertical arrows denote oscillations in pressure

The two often occur simultaneously, but are not necessarily equivalent, i.e. distortions on the extrudate can take place without flow instabilities being present, but unstable flow conditions always lead to distortions, their severity being dependent on the experimental conditions and the constitutive properties of the polymer in question. In extrusion practice the occurrence of defects marks the boundary of the commercial production rates at which polymers can be processed. Extensive reviews on instabilities in polymer flow have been published, e.g. by Tordella[10,11], Petrie and Denn[25], Vinogradov *et al.*[26], Denn[27], and recently by Larson[28] and Piau *et al.*[29].

In terms of the relevant instability and distortion effects there are two classes of behaviour which may best be introduced by the examples of linear high density polyethylene (HDPE) and long chain branched low density polyethylene (LDPE)[25]. HDPE, of course, is the polymer of our experiments to be discussed in the experimental work to follow, while LDPE, important historically, also serves to illuminate some issues relevant for general appreciation.

At the lowest rates the two classes of material behave similarly. The first appearance of extrudate distortions sets in at rates at which the upstream flow pattern is stable in both classes of material. These irregularities only affect the exterior of the extrudate and the effect itself has been referred to as 'surface melt fracture', 'loss of gloss', 'matte' or 'mattness' and in its more severe form 'sharkskin'. Here, we shall refer to it as 'surface roughness'. For HDPE the first appearance of surface roughness has been reported to be accompanied by a small change of slope of the flow curve (i.e. p vs throughput curve, usually expressed as wall shear stress and apparent wall shear rate respectively), while for LDPE the flow curve remains continuous (see for example the recent review by Piau *et al.*[29] and refs therein).

Upon increasing the rate, once an upper critical stress ($\tau_{w,UC}$) is attained, HDPE displays a flow curve discontinuity, such as shown schematically in *Figure 2*. Beyond $\dot{\gamma}_{A,crit,1}$ in *Figure 2* the stress starts oscillating and the extrudate shows periodic distortions. The flow instability responsible for this effect is referred to as 'oscillatory flow' or 'slip–stick flow'. We shall refer to it as to the appearance of the extrudate, hence we shall term it periodic bulk distortions. The stick to slip transition itself is conceivably a stress-controlled process. When a fixed pressure level is maintained a 'jump' in the flow rate occurs upon attaining $\tau_{w,UC}$. The τ_w vs $\dot{\gamma}_A$ curve will become multi-valued and a hysteresis area[16] is present*.

In both constant rate and constant pressure extrusion of HDPE, when the upper branch of the flow curve is attained, beyond a certain rate, the extrudate becomes gnarled. In the literature this type of instability has not always been clearly delineated from the one responsible for the periodic bulk distortions. Several experimental studies indicate that the instability responsible for these random effects resides in the entry orifice. This instability would be associated with rupture (cohesive failure) of the melt. The effect itself is referred to in the literature as 'waviness', 'gross melt fracture' or 'elastic turbulence'.

* It has also been reported[29] that two hysteresis areas are present in the flow curve corresponding to different values of rate. This will not concern us further

Again referring to the appearance of the extruded strand we shall term it 'gross shape distortions'.

Contrary to HDPE, LDPE does not display a discontinuity in the flow curve: τ_w keeps on rising with increasing $\dot{\gamma}_A$. Nevertheless, in addition to surface roughness already present at lower rates and stresses, gross shape distortions in LDPE set in at comparable stress values (of order 0.1–1 MPa) as in HDPE. These first take a regular helical form and become increasingly more nonuniform and uneven upon increasing the rate. There seems to be general agreement in the literature as to the site of initiation of the disturbances responsible for the gross shape distortions in LDPE being in the approach to the capillary at the entrance orifice.

Reverting to HDPE, in this case there is no conclusive attribution of the specific site of initiation of the flow instability in the extrusion system. By some views it is in the entrance. However, most studies reveal that it resides within the capillary. As regards the physical origin there are two basic views: in the first[30–33] failure of adhesion of the polymer at the capillary wall, and hence slippage at the solid boundary, is held responsible for the onset of surface roughness, and eventually leading to periodic bulk distortions. The mechanism responsible could be polymer desorption from the melt–wall interface. Here, the effect would be entirely due to the strength of the polymer–wall interface. Another way in which the violation of the stick condition at the wall can be explained is disentanglement of adsorbed and bulk chain molecules at the melt–wall interface, causing a sudden reduction of the interaction at the interface[33,34]. For the stick–slip transition to occur, this would imply that the strength of the polymer–wall interface, and hence the material of construction of the wall, be irrelevant.

By the second view[35–39], intrinsic constitutive properties of the polymer would lead to unstable flow conditions, and hence to a multi-valued flow curve. In principle, again, there are two ways in which the constitutive properties of the polymer may lead to instabilities: First, yield of the polymer material in closest vicinity to the wall, i.e. where the velocity gradient, hence shear flow rate, is maximum, may ensue as a consequence of a lower viscosity of the material near the wall compared with the bulk (shear thinning behaviour). This situation may be regarded as a slip film. Secondly, unstable flow may ensue when the rubber plateau is attained[26,38]. Once a mechanically effective network is present, which is the case in a rubber, the strains that can be imposed onto the melt are limited. In this case, primary stress build up would take place in the entry and, once the rubbery behaviour sets in, beyond some critical stress, wall slippage would occur in the capillary portion of the die.

In order to gain a ready overview of this complex subject area, we propose that, in principle, each of the above mentioned failure mechanisms could become operative at their appropriate stress level. For a given system and material the type of failure behaviour will then be determined by which of these critical stress levels is attained first. Amongst others, the differences for LDPE and HDPE could now be explained by stronger bonding at the interface for LDPE (or, alternatively, the presence of long chain branches hampering the formation of a low viscosity slip film). This would suppress adhesive failure before other sources of failure become operative, the onset of unstable flow at the entry in particular. Further, the course of the slip–stick process would then be accountable to consecutive happenings in the capillary: i) stress build up, leading to failure at the appropriate critical stress, i.e. for any of the proposed mechanisms; followed by ii) stress relief after failure; in turn leading to iii) re-establishment of the situation pertaining to stable flow, i.e. readhesion. After this a new cycle will take place.

In view of the above it will be readily apparent how these failure sources will be influenced by altering interfacial and constitutive properties. If, as a result, one of the critical failure stresses is raised (e.g. by increasing adhesion through altering the material of construction and/or wall surface topology) then the corresponding failure mode may be delayed until higher stress levels are reached. In the course of this the extruded material may stay smooth up to such higher stresses, and corresponding flow rates, or alternatively other modes of failure, may intervene. In either case, we see, that we have acquired an understanding of what is happening with the possibility of purposeful planning of the outcome of extrusion practice.

In the light of this we can also see why these irregularities are delayed under 'window' conditions: namely, by the work in parts 1 and 2 we create a new phase in close vicinity to the wall promoting slippage. As a result, at a given rate of flow, the stress (and, hence, the pressure drop over the capillary) is lowered. In the window the stress at the wall does not attain the level required to activate the agencies responsible for surface roughness (e.g. polymer fracture at the die exit) and for periodic bulk distortions (e.g. polymer desorption from the wall). Consequently stable flow can then be maintained at rates at which otherwise (i.e. at higher T) extrudate irregularities such as surface roughness and periodic bulk distortions would have occurred. The presence of the new phase relying on flow-induced chain extension is secured as long as the velocity gradient is maintained.

Scope of the paper

This final part will both entail new experimental work related to the melt fracture phenomenon also leading to some newly recognized effects involving the extrusion window. These, in addition to consolidating the views adopted in the previous parts, will further our understanding as to which of the distortions are suppressed when extrusion is conducted at temperatures within the window interval.

Specifically, the variation of capillary dimensions introduced in part 2 for temperatures pertaining to the window will be taken up further to separate entrance from capillary effects also for conventional extrusion temperatures. In order to gain further understanding on the origin of the melt flow instabilities, the relation between the pressure (stress) vs flow rate curve (flow curve) and the extrudate appearance will be scrutinized. Furthermore, the molecular weight dependence of gross shape distortions will be investigated, with the aim of designing stable flows and controlling extrudate irregularity, thereby also defining the intrinsic limitation of the window effect. Finally, with the objective of creating a flow type where conditions of slippage are established *a priori*, the role of external lubrication agents will be explored. In all the above window extrusion will be compared with extrusion at conventional temperatures.

EXPERIMENTAL

The majority of extrusion experiments were performed on a Davenport capillary rheometer (Daventest Ltd.), described in detail elsewhere[5]. These experiments were performed at a fixed rate of extrusion. Some extrusion experiments at constant pressure were also carried out using a Rheograph 2002 instrument (Göttfert). Here a constant force was maintained on the piston using a PID-control system[6]. In most extrusions short cylindrical, stainless steel capillary dies were used having a length over diameter ratio (L/D) of 7 and lengths of 14 and 10.5 mm respectively. The entrance angle was 90° (whole apex).

In order to study the influence of the presence of a capillary portion on the melt fracture phenomenon, experiments with zero-length capillary dies (orifice dies) were carried out. The orifice had a 90° entrance angle and a 120° exit aperture, and experiments were performed at temperatures both below the temperature window (146°C), where flow-induced crystallization effects are known to set in, at temperatures within the interval (151°C), and at conventional extrusion temperatures (160°C) respectively. Die swell ratios were evaluated (as the ratio of extrudate and orifice diameters) and a qualitative comparison was established with results from similar studies using capillary dies.

Extrusion experiments with an 'external' lubricating agent were conducted to study the flow behaviour at conditions where slip at the wall is known to occur (see e.g. ref. 29). The additive used was a fluoroelastomer, namely a copolymer of vinylidene difluoride and hexafluoropropylene (KYNAR FLEX 2801, $\rho = 1.78\ \mathrm{g\ cm^{-3}}$, $M_w > 10^6$ (data from supplier), $T_m = 139$°C (as determined by d.s.c. at 10°C min^{-1} heating rate)). A standard $L/D = 14/2$ stainless steel capillary die was used and the flow behaviour was examined at temperatures corresponding to the window interval (151°C) and at higher temperatures (154°C and 160°C). The polymer powder (HD6720 pr200, see *Table 1*) and the fluoroelastomer additive were mixed in a mill for several hours, prior to loading the rheometer barrel. A 2.5 wt% concentration was chosen as to ensure wetting of the metal wall of the capillary.

The materials used in the extrusion experiments were linear HDPEs of molecular weight between conventional moulding grades and ultra high molecular weight polyethylene, i.e. the weight-average molecular weights ranged from 10^5 to $10^6\ \mathrm{g\ mol^{-1}}$ as determined by gel permeation chromatography (g.p.c., see *Table 1*). The majority of experiments was carried out with a polymer having $M_w = 2.8 \times 10^5$ (HD6720 pr200, $M_w/M_n \approx 7.5$, supplied by DSM, The Netherlands). For the studies on the role of polymer molecular weight only samples with $M_w/M_n \approx 3$–6 were used in order to keep the polydispersity within well defined limits.

Samples for extrusion were prepared in the rheometer by compaction of the powder at ambient temperature and heating to 180°C (30 min) to erase any residual powder or nascent grain structure. Prior to the extrusion experiment the specimens were cooled to preselected temperatures and conditioned for at least 20 min. G.p.c. results had indicated that the procedure adopted did not lead to significant changes in the molecular weight distribution.

Table 1 High density polyethylene samples used in extrusion experiments

Sample code	M_w (g mol^{-1})	M_w/M_n	Supplier
Rigidex 006-60	1.30×10^5	5.9	BP Chemicals
LAHD 01	4.40×10^5	4.9	BP Chemicals
HD6720 pr200	2.80×10^5	7.5	DSM
A	2.62×10^5	3.1	DSM
B	3.81×10^5	5.1	DSM
C	5.08×10^5	4.3	DSM
D	7.08×10^5	6.5	DSM
E	1.0×10^6	4.2	DSM

(Experimental grades A–E have approx. 0.15 CH_3 per 1000 C atoms)

RESULTS

Observations at conventional extrusion temperatures

Figure 3 shows an (apparent) flow curve recorded at 180°C. Photography of the extruded strands corresponding to *Figure 3* is displayed in *Figure 4*. (The values for $\dot{\gamma}_A$ in *Figure 4* are indicated by the arrows in *Figure 3*. The direction of extrusion in *Figure 4* is from left to right.) In addition to measuring the pressure and examining the extrudate appearance as a function of $\dot{\gamma}_A$, the exit flow rate of the extrudate was observed visually during these experiments. When gradually increasing the flow rate, the following events are noticed:

(i) At the very lowest rates the extrudate is smooth and glossy ($\dot{\gamma}_A = 1.1\ \mathrm{s^{-1}}$ in *Figures 3* and *4* (top)). Upon increasing the rate of extrusion to $3.8\ \mathrm{s^{-1}}$ the extrudate develops fine scale surface distortions which have a screw-like appearance. These striations are perpendicular to the flow direction and become more pronounced upon increasing the rate further.

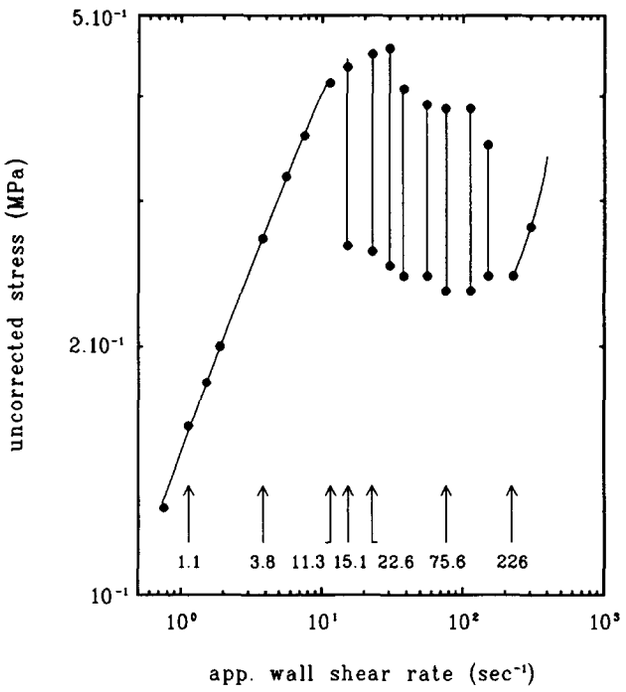

Figure 3 Flow curve for HDPE ($M = 2.8 \times 10^5$) recorded at 180°C. The vertical lines denote pressure oscillations. The arrows designate the apparent wall shear rate values for which the corresponding extrudates are shown in *Figure 4*

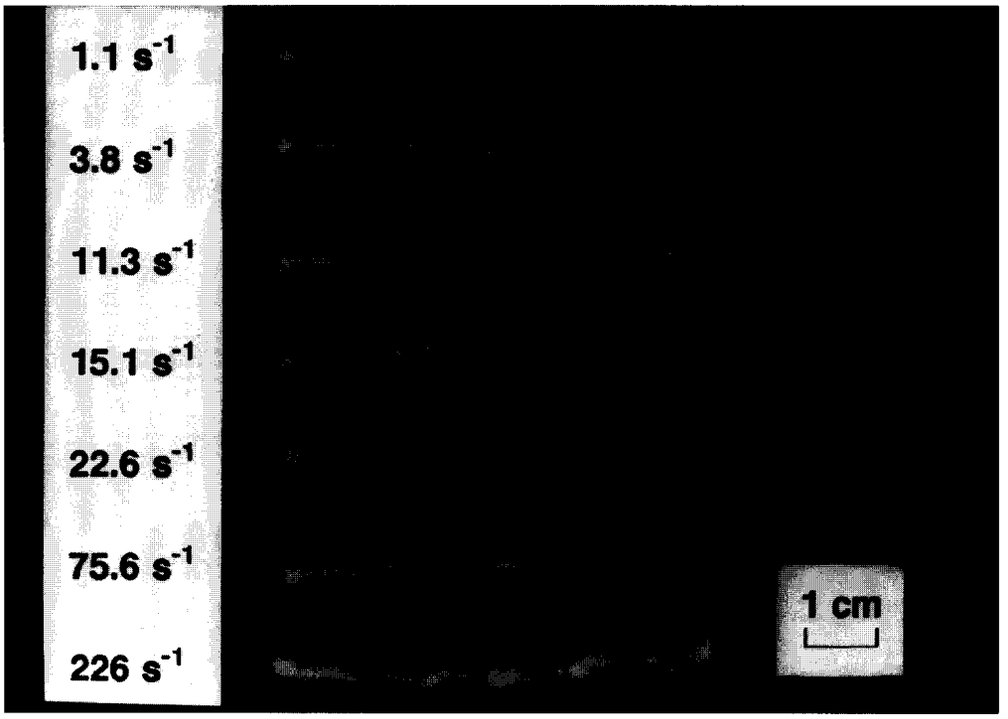

Figure 4 Photograph of extrudates produced at 180°C. Values of apparent wall shear rate correspond to arrows in *Figure 3*

(ii) When increasing the rate still further, periodic fluctuations are observed in the pressure (the range of these p oscillations are designated by vertical lines in *Figure 3*). During these p oscillations the exit flow rate of the extrudate is found to vary periodically, i.e. the melt exits in spurts. The oscillation in p itself entails a regular pattern of increasing and decreasing pressures as a function of time. More specifically, at the lower rates in this oscillatory flow regime ($\dot{\gamma}_A = 11.3\,s^{-1}$), each oscillation 'cycle' was observed to consist of three well defined stages[40]: In the first stage, i.e. in the region corresponding to an increase of pressure, there is a steady efflux of an extrudate possessing a distorted, screw-like exterior (*Figure 4* at $\dot{\gamma}_A = 11.3\,s^{-1}$; the strand shown displays three repeating units, each corresponding to an oscillation 'cycle'). At the end of this first stage, i.e. at the pressure maximum of each cycle, the flow rate suddenly increases sharply, accompanied by a smooth portion being ejected from the die. A steep drop of pressure is observed accordingly (stage 2). The portion of the smooth extrudate which emerges first (right hand side in *Figure 4*) has a diameter slightly larger than that of the final portion (left hand side in *Figure 4*) in stage 2. After this sharp drop, a third region is observed where the pressure is again decreasing, but at a rate lower than in stage 2. In stage 3 an extrudate possessing a rough surface, with fine scale striations perpendicular to the flow direction, is obtained at a comparatively high exit flow rate. The latter surface distortions are seen to be finer than the ones corresponding to the increasing pressure portion of the cycle (stage 1), and are similar to those observed at the lower rates in *Figure 4* ($\dot{\gamma}_A = 3.8\,s^{-1}$).

As can be deduced from *Figure 4* ($\dot{\gamma}_A = 11.3\,s^{-1}$) the volume of extrudate ejected when the pressure decreases during the oscillation cycle, i.e. the smooth portion (stage 2) and the portion with the fine striations (stage 3), roughly corresponds to the capillary volume*. This implies that, at the lowest rates of extrusion in the oscillatory flow regime, the stressed material in the capillary is thus expelled in its entirety[40].

(iii) At higher rates in the oscillatory flow regime ($\dot{\gamma}_A = 15.1$ and $22.6\,s^{-1}$) the number of periodic pressure changes per unit time (i.e. frequency) was observed to be enhanced. At the same time, the volume (length) of the strand extruded during (the part corresponding to decreasing p of) each oscillation cycle appears to be reduced compared with the one at lower rate (see *Figure 4* where the extruded strand shown now corresponds to seven successive cycles). Since the volume (length) of the strand extruded during each cycle is smaller than the capillary volume (length), it thus follows that removal of the stressed polymer within the capillary is incomplete. (This effect will be accounted for in Appendix I.)

At $\dot{\gamma}_A = 22.6\,s^{-1}$ in *Figure 4*, the part with the fine scale surface distortions is seen to be completely absent. When monitoring the pressure as a function of time, the oscillation cycle is now found to consist of only two stages, namely the first one corresponding to increasing p—and a distorted extrudate exterior emerging at low rate—and the final one to decreasing p—and an extruded strand possessing a smooth surface finish leaving the die at high exit rate—without the stage with slower falling p being present.

(iv) When the rate is enhanced beyond $\sim 35\,s^{-1}$,

* Since the average extrudate diameter is approximately similar to the capillary diameter (2 mm), it is readily seen from *Figure 4* that, here, the length of the smooth and the finely striated portions is similar to the capillary length (14 mm)

pressure oscillations still prevail. However, with increasing $\dot{\gamma}_A$, the amplitude of the pressure oscillations is now observed to diminish: as seen from *Figure 3*, the higher pressure level (hence upper critical stress, $\tau_{w,UC}$) decreases with $\dot{\gamma}_A$, whereas the lower pressure level (hence $\tau_{w,LC}$) remains essentially unaffected. The corresponding extrudate loses its periodic appearance and becomes grossly distorted (*Figure 4*; $\dot{\gamma}_A = 75.6\,s^{-1}$). The decrease of the amplitude of the oscillations is accompanied by an exit of fluid becoming gradually less discontinuous until at the highest rates in the oscillatory flow regime the spurting has ceased altogether.

(v) Upon increasing the rate to $226\,s^{-1}$, the pressure oscillations have totally disappeared while the output flow rate of the melt remains continuous. However, at these high rates of flow the random shape distortions of the extruded strand are becoming more pronounced (*Figure 4*: $\dot{\gamma}_A = 226\,s^{-1}$ (bottom)).

The above experiment displays all features of the extrudate irregularities as discussed in the Introduction. In the order of increasing $\dot{\gamma}_A$ these are : i) stable flow corresponding to an initially smooth extrudate, subsequently developing a rough surface; ii) oscillatory flow conditions leading to periodic bulk distortions; iii) another continuous branch of the flow curve at the highest rates corresponding to a grossly, yet randomly distorted filament.

Additionally, for the oscillatory flow regime, they have revealed two important new features, namely: 1) gross shape distortions commencing at rates at which pressure oscillations still prevail; 2) gross shape distortions at first appearance being accompanied by a reduction of the amplitude of the pressure oscillations with the output flow rate becoming increasingly more continuous. These effects were noticed for $L/D = 14/2$ capillary at 180°C (*Figures 3* and *4*), but most prominently for a slightly narrower capillary having $L/D = 10.5/1.5$ at the lower extrusion temperature of 160°C (*Figure 5*). Here, the sudden decrease of pressure maxima (hence upper critical stress $\tau_{w,UC}$) with $\dot{\gamma}_A$ during the oscillation cycles is even more conspicuous.

Observations in the window temperature interval

In *Figure 6* the flow curve obtained for the polyethylene melt is given at 151°C, i.e. corresponding to the *p*-minimum of the *p* vs *T* curve. The extrudates produced at several rates in *Figure 6* are contained in *Figure 7*. (Again, in *Figure 6* the $\dot{\gamma}_A$ values corresponding to the extrudates of *Figure 7* are indicated by arrows.) With increasing rate of extrusion the following events are noticed:

(i) At the lowest rates ($\dot{\gamma}_A = 1.1\,s^{-1}$) the extrudate exhibits a smooth surface finish and is glossy. Here, τ_w is found to increase with $\dot{\gamma}_A$ in a manner consistent with the observations made at higher temperatures (compare *Figure 3*: $\dot{\gamma}_A < 11.3\,s^{-1}$).

(ii) However, at a critical flow rate ($\dot{\gamma}_A \approx 2\,s^{-1}$ in *Figure 6*) this increasing trend is reversed. Now τ_w is found to decrease with $\dot{\gamma}_A$ until a plateau is reached. The photograph of *Figure 7* ($\dot{\gamma}_A = 15.1\,s^{-1}$) illustrates that the extrudate is still smooth and glossy—the same holds for $\dot{\gamma}_A = 30.2\,s^{-1}$—which is the opposite to the observations made at higher temperatures at which pressure oscillations set in leading to periodic disturbances of the extruded filament (compare *Figure 4*: $\dot{\gamma}_A = 15.1\,s^{-1}$).

(iii) At and beyond an upper critical rate ($\dot{\gamma}_A \approx 50\,s^{-1}$) severe gross shape distortions set in, such as the ones illustrated at $\dot{\gamma}_A = 75.6\,s^{-1}$ in *Figure 7*. These shape irregularities are similar to the ones observed for high rates of extrusion at 160°C and 180°C and their

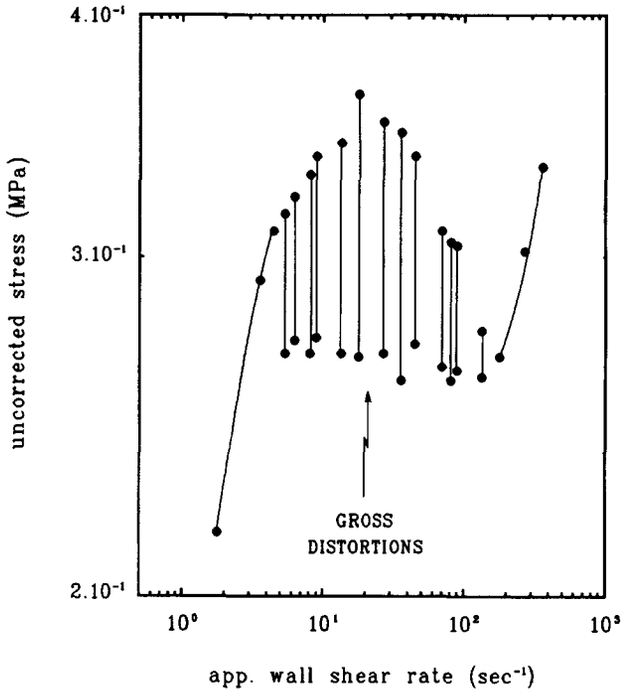

Figure 5 Flow curve for HDPE ($M = 2.8 \times 10^5$) recorded at 160°C. The vertical lines denote pressure oscillations. The arrow designates the onset of gross shape distortions

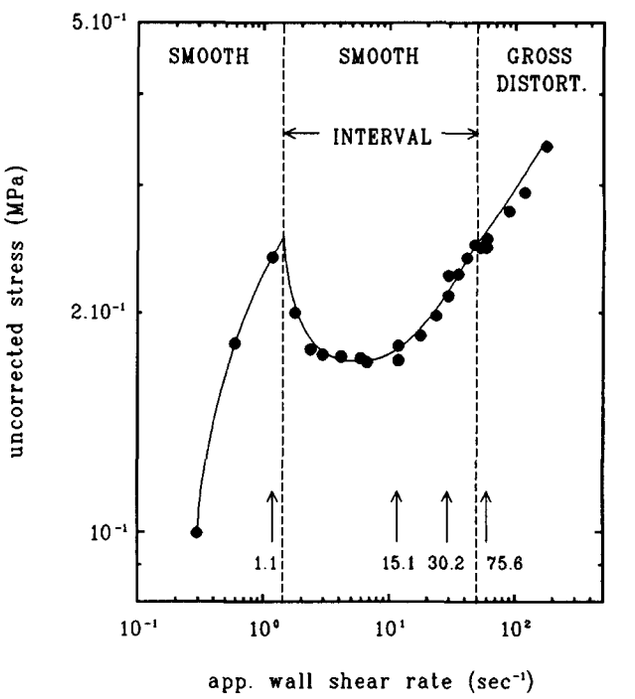

Figure 6 Flow curve for HDPE ($M = 2.8 \times 10^5$) recorded at 151°C. The apparent wall shear rate interval associated with the 'window' effect is indicated. The arrows designate the apparent wall shear rate values for which the extrudates are shown in *Figure 7*

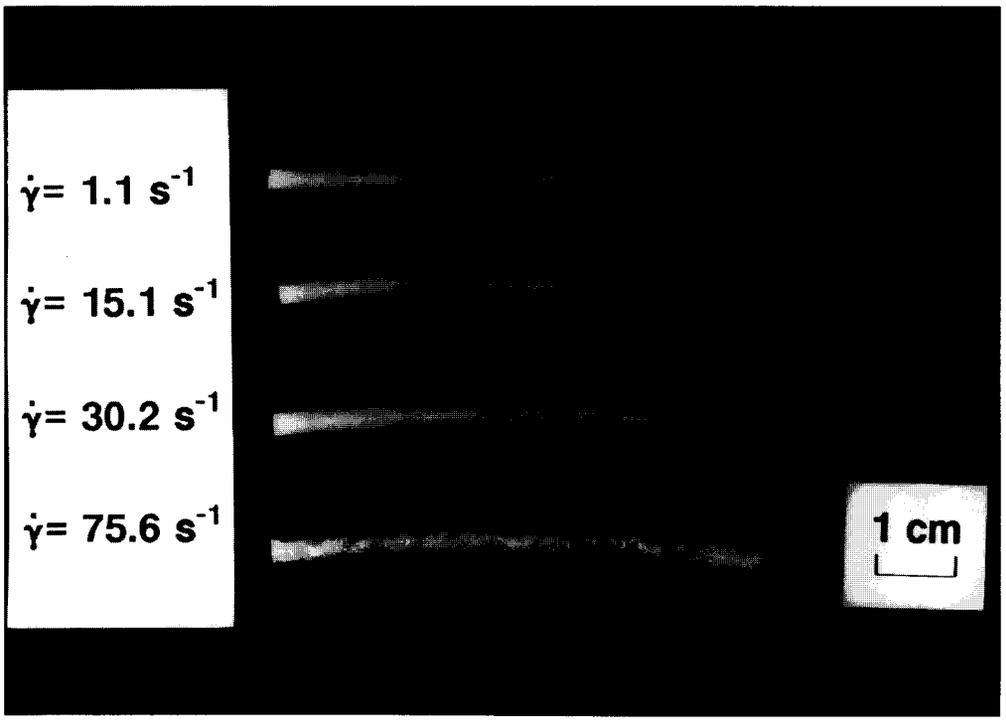

Figure 7 Photograph of extrudates produced at 151°C. Values of apparent wall shear rate correspond to arrows in *Figure 6*

inception marks the boundary of the smooth extrusion 'interval' in *Figure 6* (compare *Figure 4*: $\dot{\gamma}_A = 75.6$ and 226 s^{-1}).

The flow curve displayed by *Figure 6* (which is characteristic of all temperatures within the 'extrusion window interval' of 148–152°C) is distinct from the ones recorded at higher, more conventional temperatures of extrusion, exemplified by *Figures 3* and *5* (for $T = 180$ and 160°C respectively). First, there are no pressure oscillations and instead, there is a region of flow rates where τ_w first decreases with $\dot{\gamma}_A$, subsequently levels off to a plateau (the length of which being an increasing function of capillary length[6]), and finally increases again. Secondly, it is seen that both surface roughness effects and periodic bulk irregularities are completely absent within the extrusion window. Another difference relates to the critical (uncorrected) stress level at the onset of the window effect. It is to the latter issue that we shall turn next.

The flow experiments reported so far were conducted at fixed piston displacement rate. The results of the studies conducted at constant value of pressure (hence τ_w) are contained by *Figure 8*. (Note that *Figure 8* only shows the lower branch of the flow curves such as in *Figures 2*, *3* and *5*.) For both temperatures of 150°C ('window') and 160°C $\dot{\gamma}_A$ is seen to increase with constant stress up to a critical stress level at which a sharp discontinuity takes place. In both cases this singularity is accompanied by a manifold increase in output flow rate up to a value that was beyond the range accessible for the rheometer used and the appearance of gross shape distortions on the extrudate (indicated by arrows in *Figure 8*). It is further seen that the critical (uncorrected) stress level at the respective flow curve discontinuity is different for both temperatures: at 150°C ('window') $\tau_w \approx 0.25$ MPa, whilst at 160°C ('spurting') $\tau_w \approx 0.35$ MPa. The latter value of ~ 0.35 MPa is in full accord with the value at the onset of pressure oscillations observed in the fixed rate experiments (compare *Figures 3* and *5*). Moreover, within the range of temperatures investigated (152–220°C) this stress level was found to be independent of temperature.

Another difference noticed concerned the appearance of the extruded strand. At 160°C, except for the very lowest value tested ($\tau_w \approx 0.11$ MPa), surface roughness is present for all stress levels up to the discontinuity. On the

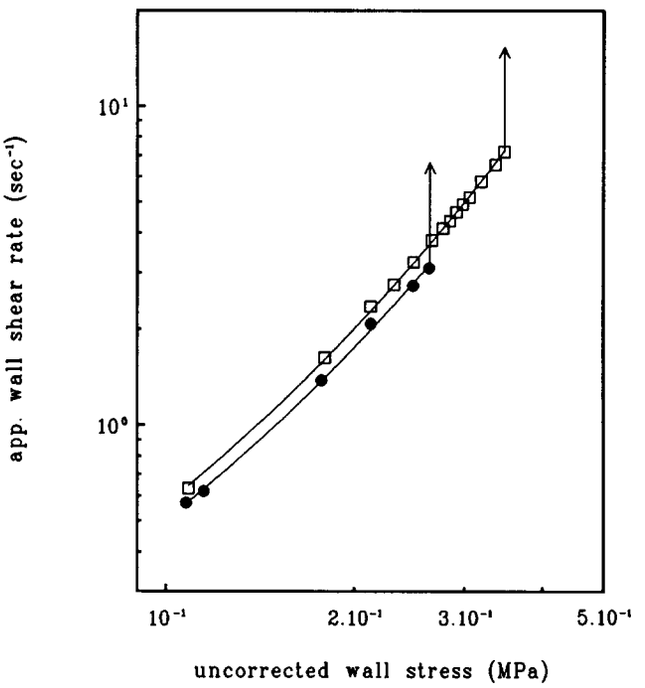

Figure 8 Flow curves for HDPE ($M = 2.8 \times 10^5$) recorded at constant pressure at temperatures of 150°C (●) ('window') and 160°C (□) respectively (Note that only the lower branch of the multi-valued flow curve as given in *Figure 2* is shown)

contrary, for the lower extrusion temperature of 150°C, a smooth and glossy extrudate is obtained for all stresses up to the singularity. These observations are in line with those made at constant rate.

Finally, for both temperatures of extrusion, upon attaining the respective critical stress level, first a smooth plug is ejected at a progressively increasing rate, which subsequently becomes gnarled when some critical throughput value is attained. The length of the smooth portion was considerably larger at 150°C.

The extrusion experiments both at fixed rate and constant stress thus reveal significant differences between operation at conventional and window temperatures. These differences become apparent both in terms of the flow behaviour (i.e. rheology) and the appearance of the extrudate.

The studies reported so far all comprised a single polymer material ($M = 2.8 \times 10^5$). Flow experiments involving different molecular weights will be reported in what follows next.

The role of molecular weight

By either of the two methods, such as underlay *Figures 1* and *6*, the onset of the window effect in terms of $\dot{\gamma}_A$, apparent as the occurrence of a minimum in p at a sharply defined T and a sharp discontinuity in the flow curve respectively, was mapped as a function of molecular weight (M) for M in the range 10^5–10^6 g mol^{-1}. A precise negative fourth power relation with M could be established, which is plotted in *Figure 9* (bottom)*:

$$\nu_c \propto \dot{\gamma}_{A,c} \propto M^{-4.0} \qquad (1)$$

By recording flow curves at Ts within the window interval, we could then determine the apparent wall shear rate at the onset of gross extrudate distortions by a visual criterion quite accurately. This is in sharp contrast to the situation at conventional temperatures of extrusion, in which case several features of irregularities were found to overlap (*Figures 3* and *5*). The critical values of $\dot{\gamma}_A$ at the inception of gross distortions obtained for several Ms at 150°C are also included in *Figure 9* (top). Despite the inevitably broad molecular weight distributions of the polyethylenes used, these data points again fall on a straight line, albeit with a much reduced slope compared to the one applying to the onset of the extrusion window effect. Accordingly, the apparent wall shear rate at the onset of gross distortions, $\dot{\gamma}_{A,g}$, is found to obey a negative 1.5 ± 0.5 power relationship:

$$\dot{\gamma}_{A,g} \propto M^{-1.5} \qquad (2)$$

Given the different power relationships displayed by equations (1) and (2), it follows that the two singularities—the window effect and the occurrence of gross shape distortions—must have widely different origins.

From equations (1) and (2) it follows further that the two lines in *Figure 9* must intersect. At intersection, $\dot{\gamma}_{A,c} = \dot{\gamma}_{A,g}$, the corresponding M (M^*) defines the limit above which the window effect leading to a smooth extrudate can be realized, and below which it cannot. Namely, for $M \geq M^*, \dot{\gamma}_{A,g} \geq \dot{\gamma}_{A,c}$, where $\dot{\gamma}_{A,g} - \dot{\gamma}_{A,c}$ defines the apparent shear rate interval for the window effect; for $M < M^*, \dot{\gamma}_{A,g} < \dot{\gamma}_{A,c}$, which means that the apparent shear rate required for the window effect yielding a smooth extrudate cannot be reached.

From *Figure 9* this critical M^* is estimated to be 10^5 g mol^{-1}. It is further seen that for $M \geq M^*$ the range of extrusion rates at which 'window flow conditions' can be realized, $\dot{\gamma}_{A,g} - \dot{\gamma}_{A,c}$, widens upon increasing M.

Orifice die experiments on extrudate irregularities

It was shown previously[6] that the window effect could not be realized when using an orifice die. This was in line with the expectation that the presence of a capillary (wall) would be a prerequisite for the window effect to occur. In the present study, orifice dies were used also to study the sequence of the various extrudate irregularities (window effects apart)—i.e. surface roughness → periodic distortions → gross distortions—occurring as a function of extrusion rate. These orifice dies were further employed to evaluate the amount of die swell. The results of these experiments are as follows: The extrudate resulting from an orifice die shows no surface roughness, and no periodic bulk distortions, yet can display pronounced gross shape distortions at the appropriate elevated flow rate when extrusion is carried out within the window interval. At conventional extrusion temperatures, surface roughness is observed already at very low rates ($\dot{\gamma}_A \approx 1$–$25\,s^{-1}$ at 160°C), becoming more pronounced upon increasing the rate and turning into gross distortions at the highest rates of extrusion ($\dot{\gamma}_A > \sim 25\,s^{-1}$ at 160°C): for orifice dies periodic bulk distortions are never displayed (i.e. oscillatory flow conditions never occur). At temperatures below the window interval none of the extrudate

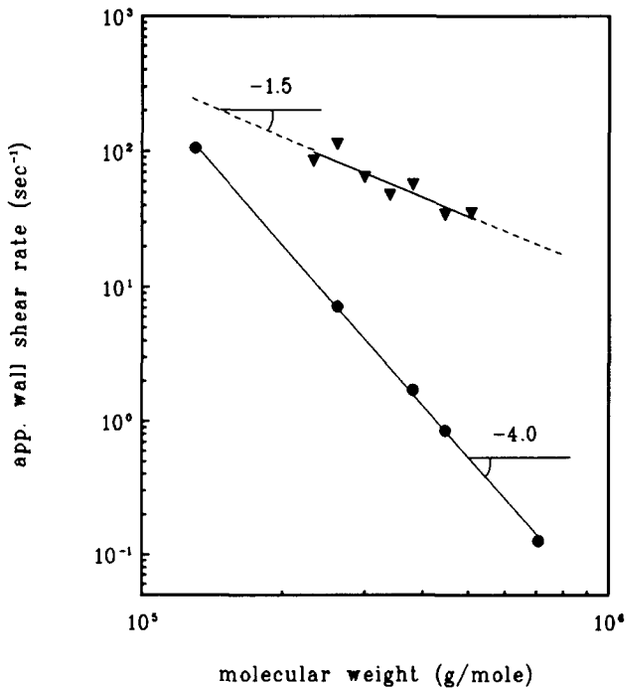

Figure 9 Critical apparent wall shear rate at the onset of the window effect (●) and gross shape distortions (▲) as a function of molecular weight

* In this paper we retain the symbols $\dot{\gamma}_A$ and τ_w to denote apparent wall shear rates and (uncorrected) wall stresses respectively as defined previously[5,6]: $\dot{\gamma}_A = 32Q/\pi D^3$, where Q = volume throughput and D = capillary diameter, and $\tau_w = \Delta p_{tot}/4(L/D)$, where Δp_{tot} = total pressure drop measured and L = capillary length

irregularities is observed. Yet, the die swell ratios are considerably higher than at conventional extrusion temperatures (see below).

Overview of extrudate irregularities

The outcome of the preceding experiences on extrudate irregularities, including capillary and orifice dies are summarized in *Table 2*. The comparisons are applied to temperatures below the window interval (T_{in}) (146°C), within the window interval (151°C) and at conventional extrusion temperatures (160°C) with the extrusion carried out at $\dot{\gamma}_A = 5\,s^{-1}$ throughout.

In accord with the expectation that the presence of a capillary enables relaxation of the strain accumulated by the melt in the constriction at the entry orifice, the die swell ratio is appreciably lower when a capillary is present. This appears to be the case at all Ts studied. At $T < T_{in}$ (146°C), extrudate irregularities such as discussed above were never observed. Instead, the extrudate exhibited considerable die swell. At the appropriate elevated flow rates the diameter of the extrudate became nearly equal to the diameter of the reservoir upstream of the constriction. Thus, at these 'low' temperatures nearly full recovery of the strain accumulated by the melt in the entrance takes place*[4].

At $T = T_{in}$ (151°C) neither capillary nor orifice die flow gives rise to surface roughness and periodic distortions. As demonstrated in previous work[5], at these temperatures, the die swell ratio is minimum. At highest rates (i.e. at $\dot{\gamma}_A > \sim 50\,s^{-1}$), however, gross shape distortions occur both for the orifice and the capillary die.

Flow experiments using a fluoroelastomer additive

The flow curves of the pure polymer (top) and polymer to which the fluoroelastomer was added (bottom) are shown in *Figure 10* for $T = 151$°C (i.e. corresponding to the p-minimum of the p vs T curve in *Figure 1*). The flow curve for the pure polymer has been taken from *Figure 6*.

In the presence of the fluoro additive, at the lowest rates ($\dot{\gamma}_A < \sim 1\,s^{-1}$), τ_w reaches an initial value which slowly decays with time elapsed (the latter effect being demonstrated by the vertical arrows). At higher rates a steady state is attained a few minutes after start-up of the flow. Accordingly, with increasing $\dot{\gamma}_A$ a narrow plateau in τ_w is observed ($\dot{\gamma}_A \approx 1$–$4\,s^{-1}$), followed by a steep rise in τ_w ($\dot{\gamma}_A > \sim 4\,s^{-1}$). Although the effect of lubrication on τ_w is prominent even for $\dot{\gamma}_A < \sim 15\,s^{-1}$, it is further seen that for the pure polymer, for $\dot{\gamma}_A$ beyond $\sim 15\,s^{-1}$, the stresses are comparable to, or even slightly smaller than, the τ_w values obtained for the lubricated flow.

At the highest rates both for the pure material and the lubricated polymer, gross extrudate distortions are found to take place. In the presence of the fluoroelastomer the critical onset shear rate was slightly higher (i.e. $\dot{\gamma}_A \approx 60\,s^{-1}$ compared with $\dot{\gamma}_A \approx 50\,s^{-1}$ for the pure polymer).

A further effect was noticed when examining the influence of temperature on the flow curves for the lubricated polymer. *Figure 11* displays the flow curves recorded at temperatures of 151, 154 and 160°C, all showing a plateau in τ_w at the lower rates of extrusion ($\dot{\gamma}_A < \sim 4\,s^{-1}$) and an increasing value of τ_w at higher $\dot{\gamma}_A$. By adding the fluoroelastomer pressure oscillations, which would otherwise have prevailed at the conventional extrusion temperatures, are fully suppressed. The entire flow curve is seen to shift to progressively lower τ_w

Table 2 Relative die swell ratios and the presence of distortion as a function of temperature for orifice dies and capillary dies

Temperature	Die type	Die swell ratio	Surface roughness	Periodic bulk distortions	Gross shape distortions
146°C	Capillary	2–3	n	n	n
	Orifice	>3	n	n	n
151°C	Capillary	1–1.25	n	n	y
	Orifice	1.25–1.5	n	n	y
160°C	Capillary	1.25–1.5[a]	y	y	y
	Orifice	1.5–2[a]	y	n	y

n = no, y = yes
[a] An estimate since surface roughness is present

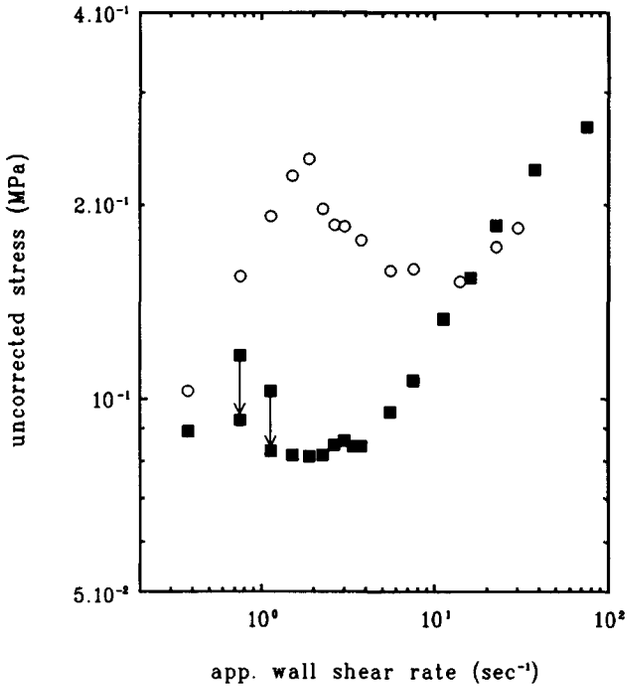

Figure 10 Flow curves recorded at 151°C for pure HDPE (○) and HDPE containing 2.5 wt% fluoro additive (■) ($M = 2.8 \times 10^5$)

* We propose that full recovery can take place since the deformed melt is 'frozen in' in the form of flow-induced fibrous crystals which prevent the melt from relaxing: Upon exit of the extrudate these fibrous crystals will melt and the elastic energy stored will be fully recovered

when increasing T. Apart from this shift, it is seen that the shape of the flow curve is invariant with temperature, also including Ts corresponding to the window interval. Through adding the lubricant, in addition to the periodic bulk distortions, surface roughness is also suppressed within the entire T regime studied. At the highest $\dot{\gamma}_A$s the only type of extrudate irregularity setting in is gross shape distortion. Nevertheless, at the window temperature, the rate at which these gross distortions first became apparent was substantially higher than for the Ts above the window interval (i.e. $\dot{\gamma}_A \approx 60\,s^{-1}$ at 151°C as opposed to $7\,s^{-1}$ and $10\,s^{-1}$ at 154°C resp. 160°C). (Note that the onset of gross shape distortions is indicated for each T by vertical arrows through the corresponding symbols in *Figure 11*.)

DISCUSSION

For all of the relevant extrudate irregularity effects—surface roughness, periodic bulk distortions and gross shape distortions—the critical onset can be postponed to higher values of rate upon increasing temperature (T) (Compare, for example, the flow curves in *Figures 3* and *6*.) This is in accord with expectation that the resistance to flow (i.e. melt viscosity) is a decreasing function of increasing T. Since the critical stress level at the onset of the irregularity appears to be insensitive to T, the first appearance of the irregularity will set in at a correspondingly higher throughput. (It is noted that, in the literature, there is ambiguity as regards the magnitude of the critical stress for the 'spurt' effect ($\tau_{w,crit}$ see *Figure 2*) as a function of temperature. Most studies indicate that the critical τ_w remains essentially unaffected by T. Others show that $\tau_{w,crit}$ is increasing with T (see, for example, ref. 33). We take the difference in T between the two extrusion temperatures studied (10°C) as too small to significantly affect $\tau_{w,crit}$.

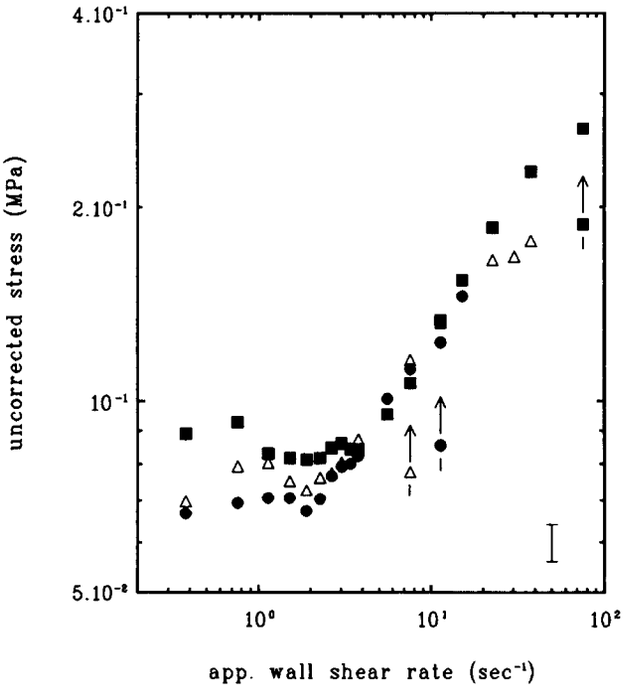

Figure 11 Flow curves for HDPE containing 2.5 wt% fluoro additive recorded at 151°C (■), 154°C (△) and 160°C (●). The arrows designate the onset of gross shape distortions at the respective temperature. A typical error bar is indicated

In contrast to increasing T, which may have several undesirable consequences such as polymer degradation and higher operation costs, the present works show that a *reduction* of T to within the 148–152°C 'window' interval can also have the effect of suppressing extrudate irregularity at rates at which they should otherwise have prevailed (compare *Figures 4* and *7*). However, the effects associated with the 'window' go much beyond: instead of delaying surface roughness (the inception of which usually marks the boundary of the commercial production rates) and periodic bulk distortions, by extrusion within the 'window', these types of irregularity can be eliminated altogether. Since smooth extrudability is accompanied by a minimum in die swell and good shape stability[6], and since it can be realized without the need to use lubricating additives, 'window' extrusion may offer significant practical advantages for the manufacture of unidirectional products such as filaments, profiles, rods and pipes.

Apart from its direct application, 'window' extrusion provides a useful tool for the appreciation of flow instabilities and extrudate irregularities. For the latter purpose we shall briefly recapitulate the results on the decomposition of the pressure (stress) values in the flow curve of *Figure 6* into the contributions from the entrance and the capillary as arrived at previously[6]. For concise presentation, the various experimental results will be categorized as to the relevant type of irregularity and will be discussed in the order: gross shape distortions, periodic bulk distortions and surface roughness respectively. The experiments with the fluoro-additive will feature additionally.

On the separation of entrance and capillary effects in the window

Clearly, the flow field in the present extrusion geometry is highly complex, being of essentially simple shear flow character within the capillary, and having both elongational and shear flow components upstream of the capillary orifice. The total pressure drop (Δp_{tot}), which is the one being measured, is compounded by the contributions of the entry (Δp_{entry}), the capillary (Δp_{cap}) and the exit (Δp_{exit}):

$$\Delta p_{tot} = \Delta p_{entry} + \Delta p_{cap} + \Delta p_{exit} \qquad (3)$$

In order to determine the capillary constituent and the pressure losses at both capillary ends ($\Delta p_{ends} = \Delta p_{entry} + \Delta p_{exit}$) the scheme of Bagley[41] was adopted (as described in detail elsewhere[6]). The results of this procedure are shown in *Figure 12* at 151°C for a capillary having $L/D = 8/2$. To recall, the end losses are seen to be a monotonically increasing function of polymer throughput (the small discontinuity occurring just beyond the onset of the window apart), whereas the capillary pressure drop continuously decreases with increasing $\dot{\gamma}_A$ beyond the critical value associated with the onset of the window effects (i.e. $\dot{\gamma}_{A,c} \approx 2\,s^{-1}$). For all $\dot{\gamma}_A$s investigated, the magnitude of the pressure drop over the capillary was found to scale linearly with capillary length (i.e. $\Delta p_{cap} \propto L$), also for conditions at which the window effects pertain (i.e. $\dot{\gamma}_A > 2\,s^{-1}$). Thus, a 'master curve' of ends corrected stress ($\tau_w \propto \Delta p_{cap}/L$) vs $\dot{\gamma}_A$ could be constructed. (In the discussion below it will be assumed that the rise of Δp_{ends} with $\dot{\gamma}_A$ (i.e. for $\dot{\gamma}_A > 2\,s^{-1}$ in *Figure 12*), is mainly due to an increase of Δp_{entry}, hence Δp_{exit} will be neglected.)

Gross shape distortions

The flow curve of *Figure 6* and the corresponding extrudates of *Figure 7* reveal that neither surface roughness effects nor periodic disturbances of the extrudates are present when the polymer is extruded from a capillary within the extrusion window interval. At the highest rates in *Figure 6*, however, gross shape distortions set in.

In general, irrespective of the flow behaviour of the melt in the capillary, gross shape distortions are expected to occur as soon as the stress in the material reaches a critical value. Since the stress in the capillary ($\tau_w \equiv \Delta p_{cap} D/4L$) in *Figure 12* is found to be a decreasing function of $\dot{\gamma}_A$ at $T = T_{in}$, whilst Δp_{entry} (Δp_{ends}, hence the stresses arising at the capillary entrance), increases monotonically with $\dot{\gamma}_A$, it follows that the origin of the gross distortions can only lie in the approach to the capillary where the flow is of predominantly elongational character, a conclusion already inferred previously[6], but here substantiated from a new angle, we maintain in a definitive manner.

Support for this contention is provided by *Figure 9*, showing that the onset shear rate for the window effect has a different dependency on weight-average molecular weight ($M_w \equiv M$) than the onset of gross distortions. Namely, the precise negative 4th power relationship of $\dot{\gamma}_{A,c}$ in M (equation (1)) is related to simple shear flow in the capillary[5,6]. The flow mechanism responsible for the negative 1.5th exponent of $\dot{\gamma}_{A,g}$ in M at the onset of gross shape distortions (equation (2)) must have a different origin, which may well be related to instabilities in the entry flow. In this respect one could envisage gross distortions arising as the consequence of stress build up in the elongational flow field upstream of the capillary leading to rupture of the polymer melt once a critical stress level is exceeded. This critical stress level may well be related to the cohesive strength of the material. A

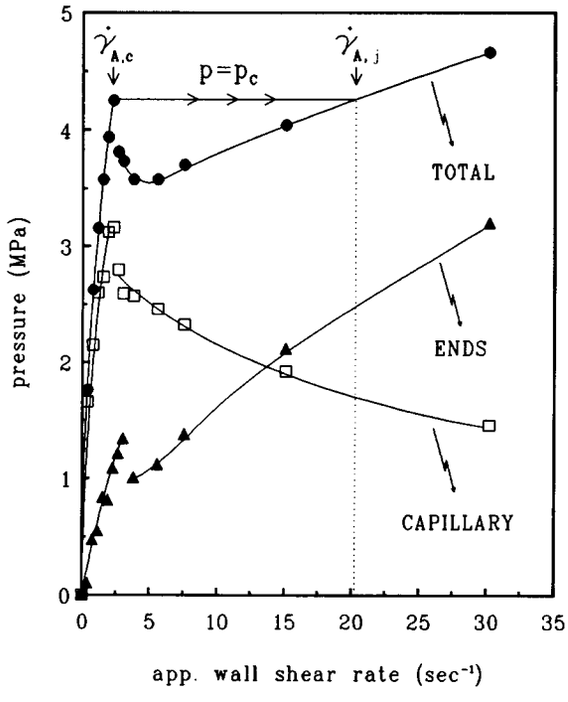

Figure 12 Decomposition of the total pressure drop (●) into end losses (▲) and capillary pressure drop (□) as a function of apparent wall shear rate to illustrate the various events that occur when maintaining a constant pressure in the rheometer (for explanation see text)

negative 1.5 power law exponent for the M dependence was observed previously in elongational flow studies, even if in a different context, namely for the critical elongational strain rate for the coil→stretch transition ($\dot{\epsilon} \propto M^{-1.5}$) of individual polymer chain molecules in dilute polymer solutions[42]. This correspondence may not be mere coincidence, and could perhaps serve as a starting point in a search for an explanation, a point which, however, we do not intend to follow up here.

At the 'cross over' point at $M^* \approx 10^5$ in *Figure 9*, the inception of gross shape distortions corresponds to the same rate which is required for the onset of the window effect (i.e. $\dot{\gamma}_{A,g} = \dot{\gamma}_{A,c}$). It follows that for $M < \sim 10^5$ the window effect cannot be reached as smooth extrusion (capillary effect) is directly followed by gross shape distortions (entry effect).

The two relationships in *Figure 9* were plotted for a fixed capillary geometry ($L/D = 14/2$ and $2\alpha = 90°$). The critical onset $\dot{\gamma}_{A,c}$ of the window effect is found to be independent of capillary length (L) and of the entrance angle (2α) of the capillary die, and nearly invariant with capillary diameter (D)[6]. In contrast, any elongational flow effect, such as held responsible for the gross distortion effect, would be strongly influenced by changes in D and 2α. It is expected that the line corresponding to the onset of gross distortions in *Figure 9* would shift to higher values of $\dot{\gamma}_A$ when the 'strength' of the elongational flow component at the entry is diminished (e.g. by increasing D at a fixed reservoir diameter, or decreasing 2α). The cross-over point in *Figure 9* would be displaced to lower M accordingly.

Finally, as both the onset of the extrusion window and gross melt fracture have different dependencies on M (equations (1) and (2)), the range of throughputs (hence $\dot{\gamma}_A$) enabling smooth extrusion is seen to widen with increasing M. For example, from *Figure 9* it is derived that the $\dot{\gamma}_A$-interval equals one decade for $M \approx 2.3 \times 10^5$ and two decades for $M \approx 6.0 \times 10^5$. With increasing M this 'processing interval' could be increased still further. This is of potential practical importance as it is the high M materials that are conventionally the most difficult ones to process. All the above illustrates the potential of the present findings in the design of stable flows and in the control of extrudate irregularity, issues to be tested in future works.

At this stage the flow curves recorded at constant pressure (hence τ_w) at the temperatures of 150 and 160°C need commenting on (*Figure 8*). Although these curves may, at first sight, seem to be largely similar, i.e. they both exhibit a discontinuity ('spurting') at some critical value of stress, the mechanisms underlying the spurt must be widely different. This stems from the fact that the singularity related to the window effect is accomplished at reduced stress (i.e. ~ 0.25 MPa as opposed to ~ 0.35 MPa). As pointed out in the Introduction, the 'spurting' effect commonly observed at the higher stress value at 160°C (and any other $T > 152$°C) we attribute to interfacial failure or constitutive instabilities, i.e. depending on the critical stress levels corresponding to these failure mechanisms. On the contrary, we assign the flow curve discontinuity observed at the lower value of stress at 150°C to the creation of a low viscosity slip film, which is the result of a flow-induced phase transformation of the melt near the capillary wall.

In both constant stress experiments of *Figure 8*, upon attaining a critical stress, first a smooth extrudate emerges at gradually increasing output flow rate, which develops gross shape distortions beyond some critical flow rate. Using the experimental evidence obtained in the constant rate experiment at temperatures pertaining to the extrusion window, it is argued in Appendix II that the onset of gross distortions can be delayed by using shorter capillary dies. (Although the way of reasoning is adopted for the particular case of the window temperature interval, we infer that it should also be applicable at conventional extrusion temperatures.)

The foregoing clearly demonstrates the usefulness of performing rheological experiments in the temperature 'window'. Namely, since other types of irregularity, which would otherwise have interfered and obscured the picture, are absent, gross melt distortions can be studied as an isolated event. By performing rheological studies within the window interval, i.e. by decomposition of the total pressure drop into capillary and entry constituent and determination of the dependency of the critical onset shear rate (throughput) on M, the origin of gross shape distortion can be attributed conclusively to the entry flow upstream of the capillary. Since the window effect was shown to be due to happenings within the capillary, we feel justified in transferring our experience on gross shape distortions, gained under window temperatures, to the higher temperatures commonly applied in extrusion practice.

Periodic bulk distortions

When oscillatory flow conditions pertain, in practice, at temperatures above the window interval, the extrudate exhibits periodic bulk distortions. Pressure fluctuations are observed only when the rheometer is operated at a fixed piston displacement rate. Conversely, when conditions of constant pressure are maintained, the throughput is seen to 'jump' between the two branches of the flow curve (see schematics of *Figure 2* and *Figure 8*), and stable flow cannot be sustained at values of throughput intermediate with respect to those corresponding to this upper and lower branch.

In the context of periodic extrudate distortions, at this stage we recall the results for the orifice die experiment conducted at conventional temperatures. Here, the sequence of extrudate irregularities was found to be different from that for capillary dies. Namely, at the lowest rates surface roughness was present which turned into gross shape distortions discontinuously beyond a certain rate of extrusion ($\dot{\gamma}_A \approx \sim 25\,s^{-1}$ at 160°C) without oscillatory flow conditions having set in previously. This suggests that the presence of a capillary is a prerequisite for the occurrence of oscillatory flow effects, which is in line with recent results reported by Piau *et al.*[43] on linear polydimethylsiloxanes. The fact that gross shape distortions are present even in the absence of a capillary portion, is in full accord with the above contention that such gross defects are caused by instabilities in the converging flow at the entry. Regarding the corresponding rate at the onset of such gross distortions at normal extrusion temperatures, the value for the orifice die ($\dot{\gamma}_A \approx 25\,s^{-1}$) was observed to be similar to the one found for the capillary die (*Figure 5*). However, it is still considerably lower than the one observed for a capillary die at window temperatures ($\dot{\gamma}_A \approx 50\,s^{-1}$).

The relation between periodic distortions and gross shape distortions

It was remarked above that, for capillary dies, at conventional extrusion temperatures (180 and 160°C—*Figures 3* and *5*), gross shape distortions set in under conditions where pressure oscillations were still present. Once such gross distortions appeared, upon increasing $\dot{\gamma}_A$, the amplitude of the pressure oscillations was found to diminish, whilst the distortions became more severe and increasingly random. At still higher $\dot{\gamma}_A$, these oscillations eventually died out and the pressure became uniform again. Within the scheme laid out in the Introduction we can understand the appearance of gross distortions still within the oscillatory flow regime; namely, it is the result of the attainment of the critical stress corresponding to the onset of gross shape distortions in the elongational flow field at the entry orifice, while pressure oscillations still pertain as a consequence of reaching some critical stress level at the capillary wall.

As another question we may ask why the pressure oscillations die out at all. Clearly, at some critical throughput—marking the upper boundary of the oscillatory flow regime—the material loses its ability to reestablish the situation prior to the stick→slip transition. That is to say, on the time-scale involved, the reverse slip→stick process can no longer take place. Inability to readhesion, of course, could pertain permanently beyond the flow curve discontinuity when the rheometer is operated at constant pressure, in which case the polymer melt is in a continuous state of slippage and pressure oscillations are never prominent. In principle, such slippage can be envisaged both as failure of the polymer–wall interface (i.e. polymer desorption) and near wall slippage. With regard to the latter, Brochard and de Gennes[34] have suggested that for scarcely populated surfaces ('weak brush') adsorbed molecules may become disentangled from those constituting the bulk. This process would be stress-induced (Brochard and de Gennes refer to it as a 'marginal state') and will lead to slip along a polymer–polymer interface. Recently Drda and Wang[33] provided evidence that analogous disentanglement of anchored and bulk chains may be present also for densely populated surfaces; such is the case for HDPE on a metallic surface. Taking this disentanglement model further, the inability of readhesion of the melt beyond a certain throughput can readily be accounted for.

When the rheometer is operated at constant rate, in the decreasing portion of the oscillation cycle stress relaxation takes place. After relaxation of the stress re-entanglement will occur at the previously created polymer–polymer interface and, hence, the interface will be re-established.

At and beyond the upper boundary of the oscillatory flow regime, we propose that, on the time-scale of the flow, re-entanglement can no longer be completed and, hence, re-establishment of the interface can no longer occur. As a consequence, stresses cannot build up any longer and continuous slippage would ensue. (In Appendix I it is argued that, upon increasing $\dot{\gamma}_A$ within the oscillatory flow regime, beyond some critical value, decompression may become incomplete. Amongst others, this would lead to partial expulsion of the extrudate from the die and explain the observation that

the plug volume becomes smaller than the capillary volume. Nevertheless, we argue that, here, the melt is still capable of re-adhesion.)

As opposed to the above discussed overlap of gross shape and periodic bulk distortions, a wide separation of the two regimes has also been reported for high density polyethylene[13,30,44]. For HDPE, for example Uhland observed that pressure oscillations die out beyond a critical rate of extrusion, giving way to a distinct region where smooth and glossy extrudates were obtained. At still higher rates gross shape distortions appeared[44]. This smooth extrusion regime (which is sometimes referred to as 'super-critical' extrusion regime) was observed for several entrance angles and capillary L/D ratios, demonstrating that its presence is governed by the constitutive properties of the material alone and not by the geometry of the capillary die employed. For the case of a separation of the regimes corresponding to periodic bulk distortions and gross shape distortions, another difference was noticed regarding the amplitude of the pressure oscillations[44]. Namely, here, the amplitude was found to be an ever rising function of extrusion rate, and a sudden decrease in the amplitude of the oscillations, such as diagnosed in our own experiments (*Figures 3* and *5*), was not observed. We therefore conclude that the sudden reduction of the amplitude is the result of fracture of the melt in the entry orifice, in turn leading to incomplete adhesion of the melt in the capillary.

Gross shape distortions may thus commence, both at rates of extrusion corresponding to the oscillatory flow regime (this work), and at rates beyond the oscillatory flow regime (refs 30 and 44). In the light of the various failure modes leading to extrudate distortion discussed in the Introduction, i.e. failure of adhesion (by polymer desorption or the formation of a disentanglement layer) or constitutive instability (formation of a low viscosity slip film or through elastic behaviour), it follows that two polymeric materials of closely similar chemical constitution may possess largely different stress thresholds for the onset of the various extrudate irregularities.

At this point a further comment on the relation between the 'super critical' extrudability and our own 'window' effect needs to be made. The consequences of the two effects are similar both leading to a smooth extrudate as long as the conditions pertaining to the flow at the entry orifice are stable. In our view both effects are manifestations of plug flow, i.e. slippage at the solid wall. Yet, the conditions giving rise to the two effects are widely distinct: Those in the 'window' effect are fully defined and understood as described in these papers. Those in the 'super critical' extrusion phenomenon are unpredictable and, even in the HDPE class, are dependent on the particular material used. As opposed to the 'window' effect, 'super critical' extrudability is not confined to a specific temperature range and can occur over a wide range of extrusion rates or not at all: the material used for the study of our 'window' effect did not display it. The relation between the two effects, if any, invites further exploration.

Surface roughness

So far, the subjects of investigation have been gross extrudate irregularities and periodic bulk defects. Next, the final issue related to the melt fracture phenomenon will be addressed, namely surface roughness. In the flow curve recorded at 180°C (*Figure 3*) surface roughness was found to set in beyond some critical value of $\dot{\gamma}_A$ ($\approx 2\,s^{-1}$, see *Figure 4*) at conditions where the pressure (hence wall stress, τ_w) was uniform and an increasing function of $\dot{\gamma}_A$, i.e. in accord with most observations in the literature. In line with most experimental studies, the onset $\dot{\gamma}_A$ was found to shift to increasingly higher values with increasing temperature (compare for example *Figures 3* and *5*), whilst the corresponding τ_w remained essentially unaffected. However, when the temperature was lowered to values within the window interval, such surface roughness effects vanished altogether (*Figures 6* and *7*).

In the literature two different basic views prevail regarding the mechanism responsible for surface roughness. The first view[18,43,45–49] relates to fracture of the polymer at the die exit due to the abrupt change in boundary conditions. In the second view[30–32] the onset of surface irregularities (and, subsequently, the more severe type of periodic bulk distortions) is assumed to be caused by the occurrence of slippage in the capillary land portion of the die.

The orifice die experiments conducted at 160°C reveal that surface distortions are present even when the capillary is absent (*Table 2*). It is worth recalling that such surface roughness effects are also manifest in constriction-free flow[6], even on the comparatively large scale of the barrel of the rheometer ($d = 12$ mm) in a 'tube flow' experiment carried out at $T = 160$°C, thus demonstrating that surface roughness also occurs in the absence of a constriction. The results of these orifice and tube flow experiments both have one feature in common, namely that an abrupt change in boundary conditions takes place on exit from the flow system. Namely, both for the orifice die and the parallel rheometer barrel a considerable change in velocity takes place in the outer layer of the extrudate when the melt leaves company with the walls in the particular flow geometry. It is conceivable therefore that acceleration of material in the surface layer may give rise to high stretching forces, which may eventually lead to rupture of the material in the exterior of the extrudate.

The above experiments on the special geometries of the orifice and the tube[6], combined with general experience from capillary dies (i.e. all cases where surface roughness is prominent), thus indicate that the surface distortions in question would ensue independent of the manner in which stress build-up (i.e. the nature of the stress field) takes place prior to the change of the boundary conditions at the respective exits. Rather, they suggest that the single requirement for the onset of surface roughness is the attainment of a critical stress level at the duct exit. As regards the mechanism responsible, the present observations thus make a strong point for the view that surface roughness is caused by fracture of the polymer surface at the exit.

On the absence of periodic bulk distortions and surface roughness in the window

Probably the most conspicuous finding within the present works on polymer melt flow instabilities is the observation that the flow curve recorded at temperatures within the 148–152°C interval (T_{in}) does not display the oscillatory flow regime as discussed in the foregoing, but instead, exhibits a portion where the pressure (stress) is first seen to decrease, subsequently to bottom out as to form a plateau, and finally to rise with increasing apparent wall shear rate ($\dot{\gamma}_A$) (compare, for example,

Figures 3 and *6*). In what follows the question of the origin of this difference will be addressed.

As shown conclusively in previous works[5,6] the prime effect responsible for the reduced flow resistance associated with the extrusion window resides within the capillary portion of the die. Since a reduction of flow resistance was only observed within the sharply defined temperature interval of 148–152°C, the effect was attributed to a thermodynamic factor, a phase transformation in particular. The transformation itself would take place at a site in the (simple shear) flow field of the capillary where extension of the macromolecules is maximum. Namely, chain extension would be a precondition for such a phase transition and this would be feasible when the molecules are anchored to the wall. Considering the sharpness of the temperature interval (148–152°C), this would reflect the range of temperatures where the newly formed phase would be stable. As this phase would have to be capable of reducing the flow resistance at or close to the wall of the capillary, the highly mobile hexagonal form of polyethylene was proposed for this phase.

As confirmed by *in situ* X-ray studies[7], the rheological effect of the extrusion window, i.e. slip, is thus associated with an underlying structural process, namely a phase transformation of the melt along the capillary wall. Once this newly formed phase is present, it is not inconceivable that a disentanglement process of anchored chains from those within the bulk would be greatly facilitated and that slippage will ensue in close proximity to the solid boundary. The stick→slip transition associated with the window phenomenon is also a stress-controlled one[5,6], but, through the presence of the mobile hexagonal phase, the critical stress level itself is significantly lower than that for the common slippage effect at higher temperatures.

The presence of the hexagonal phase would further prevent stress concentration at the die exit such as would lead to high stretching forces in the material, eventually leading to surface distortions of the extrudate. The fact that stress can no longer accumulate while the material is travelling downstream the capillary, would also explain why oscillatory flow conditions, such as leading to periodic extrudate defects, do not appear under the conditions of the extrusion window.

Flow experiments using a lubricating additive

During polymer processing operations in the melt, lubricants may be added for at least two different reasons: In the first place they may be used to lower the viscosity of the polymer, hence to promote the flow of the melt. The type of compound to be used has to be (at least partially) compatible with the polymer and is usually referred to as an 'internal lubricant'.

Additives may also be used to reduce the flow resistance at the solid boundary. Sometimes coatings are applied to lower the surface tension of the die wall material,which is usually a metallic surface. By virtue of a reduction of the surface tension of the confining boundary, adhesion of the polymer would be diminished and hence the polymer molecules may slide more readily along the coated surface. Also, or alternatively, such a coating may hamper anchoring of polar functional groups of the polymer to the oxidized metal surface. Low viscosity additives are also used with the aim of confining shear deformation to a thin layer constituted by the additive at the wall. The compounds employed for these latter purposes are incompatible with the melt and are commonly referred to as 'external lubricants'. In this work experiments were conducted with such added external lubricant, more specifically, a copolymer of vinylidene—difluoride and hexafluoropropylene.

Through the addition of the fluoroelastomer, surface roughness effects as well as periodic bulk distortions, ensuing from oscillatory flow conditions, could be eliminated completely. Similar effects have also been reported in the literature when using fluorinated additives[32], fluoroelastomers[47], fluorinated powders[50], polytetrafluoroethylene capillaries[26,29] or carefully prepared surfaces containing fluorine groups[51].

In our scheme the absence of surface and periodic distortions would be accountable for in terms of a reduction of the wall stress through the presence of the fluoroelastomer along the solid boundary. As a consequence, the power requirement for extrusion would be lowered and the critical stress level for the relevant types of distortions would not be attained.

For the pure polymer, upon increasing $\dot{\gamma}_A$, the extrusion window effect at 151°C is found to set in beyond a rate of $\sim 2\,s^{-1}$ (top curve in *Figure 10*). During flow of the polymer in the presence of the fluoroelastomer additive, instead, a narrow region ($\dot{\gamma}_A \approx 0.4$–$4\,s^{-1}$; bottom curve in *Figure 10*) is observed where extrusion pressures are consistently lower than the ones observed for the pure polymer. Increasing the flow rate in this plateau region does not result in higher (wall) stresses, which can be explained by the occurrence of slippage. Namely, with increasing throughput, the slip velocity at the wall increases whilst the magnitude of the velocity gradient within the melt interior remains unaffected. In the presence of the external lubricant this slippage could be envisaged as a large velocity gradient in a very thin layer of low viscosity additive material. When the thickness of such a film is small compared with the diameter of the flow channel, it can be treated mathematically in a similar way as for the case of pure, macroscopic slippage.

Upon increasing $\dot{\gamma}_A$ further the pressure is seen to rise in a similar way as for the pure polymer at temperatures within the window interval: It is seen from *Figure 10* that the differences in pressure levels between the pure and the lubricated polymer flow types become increasingly smaller. Most conspicuously, within the interval of $\dot{\gamma}_A \approx 15$–$60\,s^{-1}$ the melt flow resistance (i.e. the ratio of the pressure and the rate) of the pure polymer becomes equal to, or even slightly lower than (i.e. the traces cross over), its lubricated counterpart.

As implied by equation (3), the total pressure drop (Δp_{tot}) is constituted by the pressure drop over the capillary (Δp_{cap}) and by the losses at the capillary ends (Δp_{ends}). As shown in previous work[6] and displayed again by *Figure 12*, when conditions for the extrusion window pertain, the decrease of Δp_{tot} observed is accounted for by a reduction of Δp_{cap}. That is to say, the window effect is associated with a reduction of the flow resistance in the capillary.

The reversal of the decreasing trend of Δp_{tot} with $\dot{\gamma}_A$ at the end of the narrow lower plateau region in *Figures 6* and *12* ($T = T_{in}$) is associated entirely with an increase of Δp_{ends}. (The presence of the hexagonal phase[7,52], when only in small amounts, is expected to have little effect on the flow resistance in the entry orifice[6]. Similarly, the

presence of the fluoroelastomer would not affect Δp_{ends} significantly since changes in Δp_{ends} will be governed by changes in elongational viscosity.)

Since the magnitude of Δp_{tot} in this portion (say at $\dot{\gamma}_A > \sim 10\,s^{-1}$ in *Figure 10*) of the flow curve is nearly similar both for the pure and the lubricated polymer at 151°C, it follows that the flow resistance in the capillary under window and lubricated flow conditions must also be largely similar. Within the window interval we have thus created flow conditions that highly resemble those when an external lubricant is present, which thus we may term 'self-lubrication'. Unlike the window effect, which is confined to a narrow temperature interval, the lubricating effect of the fluoroelastomer displays a smooth continuity in temperature (*Figure 11*). Nevertheless, extrusion in the window offers the intrinsic practical advantages of not requiring such costly and time-consuming application of additives. Window extrusion further enables production of extrudates that are free from irregularities up to higher values of throughput. Of course this raises another important question, namely the influence of window extrusion on the solidified final product. This, however, is beyond the scope of the present work.

CONCLUSIONS

When capillary extrusion of high density polyethylenes is conducted at temperatures within the sharply defined 'window' temperature interval (T_{in}) of 148–152°C, both surface roughness and periodic bulk distortions are absent. However, at the highest rates smooth extrudability is bounded by the onset of gross shape distortions. The inception of these gross shape distortions is registered at a value of pressure (stress) in the die entrance which is similar to that at higher, i.e. conventional, processing temperatures, but at a significantly enhanced throughput rate.

As verified by concurrent *in situ* X-ray studies in previous work[7,52] this 'window' effect is the consequence of a phase transformation at the particular temperature—the mobile hexagonal form of polyethylene is proposed—originating from flow-induced extension of chain molecules. The 'window' effect results when this new phase arises from chains that are adsorbed at or are in close vicinity to the wall.

Regards the issue of extrudate irregularity, comprising, by the present classification: surface roughness, periodic bulk distortions and gross shape distortions, the extrusion experiments both within the window interval and at conventional temperatures ($T > 160$°C) have led to the following conclusions:

1) By separating the entry (ends) and capillary contributions at $T = T_{in}$ (Bagley analysis) the origin of gross shape distortions can be attributed conclusively to happenings in the converging flow field at the die entrance, adding significantly to previous indications on this point.
2) As the existence of the window enables investigation of gross distortion as an effect in isolation without the interference of surface roughness and periodic bulk distortions, its critical onset could be established unambiguously. Accordingly, the critical onset apparent wall shear rate, $\dot{\gamma}_{A,g}$, obeys a negative 1.5 power law relationship in molecular weight (M): $\dot{\gamma}_{A,g} \propto M^{-1.5}$. Since the onset of the window effect has a stronger dependency in M ($\dot{\gamma}_{A,c} \propto M^{-4.0}$), the two functions must intersect. This implies that below a critical M ($M^* \approx 10^5$) the window effect is unrealizable. This M^* value is likely to be affected by the extensional flow behaviour of the specific polymer in question and therefore by the die geometry, yet to be investigated.
3) Capillary flow data at $T = T_{in}$ and orifice flow experiments at $T > T_{in}$ have corroborated the view that oscillatory flow conditions leading to periodic bulk distortions of the extrudate are confined to the capillary portion of the die.
4) Capillary flow studies at $T > T_{in}$ show that gross shape distortions may take place within a range of extrusion rates where oscillatory flow conditions also pertain. It has also been reported elsewhere[44] that gross distortions arise at rates much beyond the range where periodic bulk distortions are observed. The fact that the periodic bulk distortion and gross shape distortion regimes can either overlap or be widely separated, according to circumstances, further substantiates the view that both events have different origins, which by the presently adopted method can now be rationalized.
5) Capillary extrusion experiments at constant stress reveal a singularity in the flow curve manifest as a jump in flow rate beyond a critical stress level. This takes place both for temperatures within T_{in} and above. Since the critical stress level for the window effect ($\tau_w = 0.25$ MPa) is lower than the one associated with the onset of the 'spurting' effect at any $T > T_{in}$ ($\tau_w = 0.35$ MPa) the origin of the window effect must be different from the spurting effect at conventional temperatures.
6) Flow studies carried out in the presence of an external lubricating additive (fluoroelastomer) show that the simple shear flow behaviour of the pure polymer at T_{in} closely resembles the one of the lubricated polymer, hence corresponds to a kind of 'self-lubrication'. However, the window effect takes place even in the absence of additives and the rates at which smooth and glossy extrudates can be produced extend to beyond those for the externally lubricated polymer.
7) More generally, the above findings fall readily and supportingly into a scheme by which the variety of flow instabilities and extrudate irregularities can be profitably categorized, analysed and investigated further: namely by noting the stress criticalities which pertain to the respective underlying causes, which, as it is hoped, the present work has helped to identify.

REFERENCES

1 Waddon, A. J. and Keller, A. *J. Polym. Sci.* 1990, **28,** 1063
2 Narh, K. A. and Keller, A. *Polymer* 1991, **32,** 2512
3 Narh, K. A. and Keller, A. *J. Mater. Sci. Lett.* 1991, **10,** 1301
4 Waddon, A. J. and Keller, A. *J. Polym. Sci. Part B: Polym. Phys.* 1992, **30,** 923
5 Kolnaar, J. W. H. and Keller, A. *Polymer* 1994, **35,** 3863
6 Kolnaar, J. W. H. and Keller, A. *Polymer* 1995, **36,** 821
7 Kolnaar, J. W. H., Keller, A., Seifert, S., Zschunke, C. and Zachmann, H. G. *Polym. Commun.* 1995, **36,** 3969
8 van der Vegt, A. K. and Smit, P. P. A. *Adv. Polym. Sci. Techn., Soc. Chem. Ind.,* 1967, monograph **26,** 313

9 Nason, H. K. *J. Appl. Phys.* 1945, **16,** 338
10 Tordella, J. P. *Trans. Soc. Rheol.* 1957, **1,** 203
11 Tordella, J. P. *Rheol. Acta* 1958, **1,** 216
12 Tordella, J. P. *J. Appl. Polym. Sci.* 1963, **7,** 215
13 Tordella, J. P. 'Rheology', (Ed. F. R. Eirich), Vol. 5, Academic Press, New York, 1969
14 Spencer, R. S. and Dillon, R. E. *J. Colloid Sci.* 1948, **3,** 163
15 Spencer, R. S. and Dillon, R. E. *J. Colloid Sci.* 1949, **4,** 214
16 Bagley, E. B., Cabott, I. M. and West, D. C. *J. Appl. Phys.* 1958, **29,** 109
17 Clegg, P. L. in 'The Rheology of Elastomers' (Eds P. Mason and N. Wookey), Pergamon Press, New York, 1958, p. 174
18 Bagley, E. B. and Schreiber, H. P. *Trans. Soc. Rheol.* 1961, **5,** 341
19 Howells, E. R. and Benbow, J. J. *Trans. Plast. Inst.* 1962, **30,** 240
20 Sabia, R. and Mullier, M. E. *J. Appl. Polym. Sci.* 1962, **VI,** S42
21 Benbow, J. J. and Lamb, P. *SPE Trans.* 1963, **January,** 7
22 Lupton, J. M. and Regester, J. W. *Polym. Eng. Sci.* 1965, **October,** 235
23 Vinogradov, G. V. and Ivanova, L. I. *Rheol. Acta* 1967, **6,** 209
24 Vinogradov, G. V. and Ivanova, L. I. *Rheol. Acta* 1968, **7,** 243
25 Petrie, C. J. and Denn, M. M. *AIChE J.* 1976, **22,** 209
26 Vinogradov, G. V., Protasov, V. P. and Dreval, V. E. *Rheol. Acta* 1984, **23,** 46
27 Denn, M. M. *Ann. Rev. Fluid Mech.* 1990, **22,** 13
28 Larson, R. G. *Rheol. Acta.* 1992, **31,** 213
29 Piau, J. M., El Kissi, N. Toussaint, F. and Mezghani, A. *Rheol. Acta* 1995, **34,** 40
30 Kalika, D. S. and Denn, M. M. *J. Rheol.* 1987, **31,** 815
31 Kurtz, S. J. 'Adv. Rheol. (Proceedings IX Int. Congress Rheology)' (Eds B. Mena, A. Garcia-Rejon and C. Rangel-Nafaile), Vol. 3, Univ. Nacional Autonoma, Mexico, 1984
32 Ramamurthy, A. V. *J. Rheol.* 1986, **30,** 337
33 Drda, P. P. and Wang, S. Q. *Phys. Rev. Lett.* 1995, **75,** 2698
34 Brochard, F. and de Gennes, P. G. *Langmuir*, 1992, **8,** 3033
35 Huseby, T. W. *Trans. Soc. Rheol.* 1966, **10,** 181
36 Vinogradov, G. V., Insarova, N. I., Boiko, B. B. and Borisenkova, E. K. *Polym. Eng. Sci.* 1972, **12,** 323
37 Slemrod, M. and Hunter, J. K. *Phys. Fluids* 1983, **26,** 2345
38 Vinogradov, G. V., Malkin, A. Ya., Yanovskii, Yu. G., Borisenkova, E. K., Yarlykov, B. V. and Berezhnaya, G. V. *J. Polym. Sci. Part A-2* 1061 1972, **10**
39 Vinogradov, G. V. *Rheol. Acta* 1973, **12,** 273
40 Weill, A. *J. Non-Newton. Fluid Mech.* 1980, **7,** 303
41 Bagley, E. B. *J. Appl. Phys.* 1957, **28,** 624
42 Keller, A. and Odell, J. A. *Colloid Polym. Sci.* 1985, **263,** 181
43 Piau, J. M., El Kissi, N. and Tremblay, B. *J. Non-Newton. Fluid Mech.* 1990, **34,** 145
44 Uhland, E. *Rheol. Acta* 1979, **18,** 1
45 Benbow, J. J., Brown, R. N. and Howells, E. R. 'The Flow of Elastic Liquids at Room Temperature', Phénomènes de Relaxation et de Fluage en Rhéologie Non-lineaire, Centre National de la Récherche Scientifique, Colleque XCVIII, Paris, France 1961, p. 65
46 Cogswell, N. F. *J. Non-Newton. Fluid Mech.* 1977, **2,** 37
47 Moynihan, R. H., Baird, D. G. and Ramanathan, R. *J. Non-Newton. Fluid Mech.* 1990, **36,** 255
48 Sornberger, G., Quantin, J. C., Fajolle, R., Vergnes, B. and Argassant, J. F. *J. Non-Newton. Fluid Mech.* 1987, **23,** 123
49 Tremblay, B. *J. Rheol.* 1991, **35,** 985
50 Hatzikiriakos, S. G. and Dealy, J. M. *J. Rheol.* 1991, **35,** 497
51 El Kissi, N., Leger, L., Piau, J. M. and Mezghani, A. *J. Non-Newton. Fluid Mech.* 1994, **52,** 249
52 van Bilsen, H. M. M., Fischer, H., Kolnaar, J. W. H. and Keller, A. *Macrom.* 1995, **28,** 8523
53 Myerholtz, R. W. *J. Appl. Polym. Sci.* 1967, **11,** 687

APPENDIX I

On the periodicity of periodic extrudate distortions

It was noticed in the description of the flow curve at 180°C above (*Figure 3*) that, at lower rates in the oscillatory flow regime, the volume of the extruded strand (V_{plug}) during the decompression part of each cycle is similar to the volume contained by the capillary (V_{cap}), which is the normal observation[30,40]. Here, the oscillation cycle was found to consist of three well defined stages. However, at the higher rates in this regime V_{plug} became significantly smaller than V_{cap} and only two out of three stages remained within each oscillation cycle. In this Appendix an attempt will be made to explain the reduced volume of the extruded plug.

In *Figure A1* a double logarithmic plot is given showing the period of the oscillation cycle as a function of the apparent wall shear rate ($\dot{\gamma}_A$). It is seen that the logarithm of the total period of each cycle (t_{cycle}) is linearly dependent on the logarithm of $\dot{\gamma}_A$: $t_{cycle} \propto \dot{\gamma}_A^{-1.34}$ (which means that when, for example, the rate of extrusion is doubled, the cycle period is reduced by a factor $2^{-1.34} \approx 0.395$, i.e. it is more than halved). As laid out previously this oscillation cycle comprises a part in which stresses build up (compression) and a portion where the stress decreases (decompression). Although it has been reported that the distribution of time spent during stress build-up resp. stress release within each cycle may be weakly dependent on $\dot{\gamma}_A$ itself[53], this small effect will be neglected in the present discussion. Thus the time required for the stress to become released during each cycle will be taken to be proportional to the total cycle time (i.e. $t_{decompr.} \propto t_{cycle} \propto \dot{\gamma}^{-1.34}$).

The time required to extrude the stressed plug from the capillary ($t_{extr.}$) will have a different dependence on $\dot{\gamma}_A$. Based on common experience that e.g. upon doubling the throughput, the average residence time of the material in the capillary is halved, the extrusion time will scale inversely proportionally with $\dot{\gamma}_A$, i.e. $t_{extr.} \propto \dot{\gamma}_A^{-1}$. As $t_{decompr.}$ varies more steeply with $\dot{\gamma}_A$ than $t_{extr.}$, the two relationships must cross over. Beyond this cross-over point ($\dot{\gamma}_A = \dot{\gamma}_A^*$) the part of the oscillation cycle corresponding to decompression becomes smaller than the time required for expulsion of the plug, and hence the smooth plug will not be ejected in its entirety. V_{plug} will be smaller than V_{cap} accordingly.

(In the above assertion only the influence of extrusion rate on the period of oscillation $t_{decompr.}$ was considered.

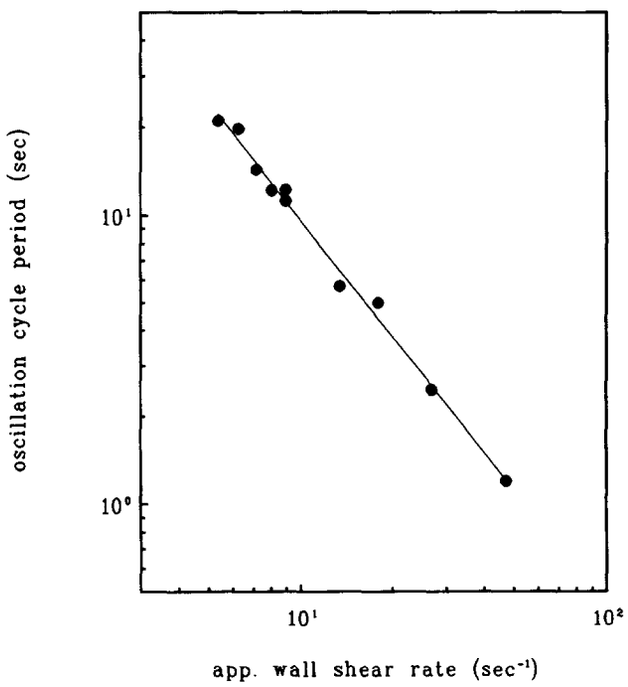

Figure A1 Oscillation cycle period as a function of apparent wall shear rate for oscillatory flow conditions ($T = 160°C$, $M = 2.8 \times 10^5$, capillary: $L/D = 10.5/1.5$)

Besides $\dot{\gamma}_A$ the cycle period appears to be influenced by the volume of the melt (V_{melt}) under the piston in the reservoir[22,40,53]. As suggested by Weill[40], for sufficiently small values of V_{melt} similar 'cross-over' conditions as above may be attained leading to partial removal of the plug. Since a reduced plug volume in the present experiment is first observed at a critical rate of extrusion ($\dot{\gamma}_A^* \approx 20\,s^{-1}$), it is inferred that the effect is most probably due to the 'extrusion rate effect', i.e. due to a 'cross-over' of the respective $t_{decompr.}$ and $t_{extr.}$ relationships in $\dot{\gamma}_A$. Although the melt volume under the piston will also affect the oscillation period (and hence $t_{decompr.}$), here this 'melt depth effect' is only of secondary importance. Moreover, with regard to the magnitude of the melt volume involved at the inception of the reduced plug volume effect (which is typically $5\,cm^3$ in *Figure 3*), this is most probably still too large for the 'melt depth effect' to set in.)

APPENDIX II

On the capillary length dependence of the onset of gross shape distortions

In this Appendix we shall show that, during the spurt effect at constant pressure, the appearance of gross shape distortions is governed by the capillary length. To this end we, again, take up the scheme displayed by the constant rate experiment of *Figure 12*. Upon increasing the rate the window effect becomes apparent as a sharp drop in pressure defining $\dot{\gamma}_{A,c}$. At still higher rates gross distortions are first diagnosed beyond some critical $\dot{\gamma}_A$, termed $\dot{\gamma}_{A,g}$, thus defining an interval $\dot{\gamma}_{A,g}-\dot{\gamma}_{A,c}$ in which extrusion is accompanied by a smooth and glossy product.

As laid out in our scheme in the Introduction, gross shape distortions will take place at and beyond a critical value of stress. Such a stress criticality can only set in in that part of the flow field where stresses are rising with increasing $\dot{\gamma}_A$. It is seen from *Figure 12* that such a situation is present only in the converging flow field at the entry orifice: namely, beyond $\dot{\gamma}_{A,c}$ the entry pressure drop (taking $\Delta p_{ends} \approx \Delta p_{entry}$) increases with $\dot{\gamma}_A$ whilst, on the contrary, the capillary pressure drop (Δp_{cap}) displays a decreasing trend in $\dot{\gamma}_A$. This critical stress level at the entry orifice will thus correspond to a critical value of Δp_{entry}, say $(\Delta p_{entry})_c$.

When a fixed pressure level is maintained, upon increasing the pressure ($p = \Delta p_{tot}$), once a critical pressure level (p_c) is attained, a 'jump' in output flow rate (hence $\dot{\gamma}_A$ will take place from $\dot{\gamma}_{A,c}$ to $\dot{\gamma}_{A,j}$ (i.e. where the line $p = p_c$ intersects the p vs $\dot{\gamma}_A$ curve in *Figure 12*). During this 'jump' Δp_{cap} and Δp_{entry} are seen to fall and rise respectively.

Depending on the value of Δp_{entry} at the end of the 'jump' (i.e. at $\dot{\gamma}_{A,j}$) the criterion for the onset of gross shape distortions $(\Delta p_{entry})_c$ may be satisfied either at 'transient conditions', i.e. *along* the jump from $\dot{\gamma}_{A,c}$ to $\dot{\gamma}_{A,j}$, or *afterwards* (i.e. at $\dot{\gamma}_A > \dot{\gamma}_{A,j}$). Thus, if $\Delta p_{entry} > (\Delta p_{entry})_c$ at $\dot{\gamma}_{A,j}$, gross distortions will ensue at 'transient conditions', whereas if $\Delta p_{entry} < (\Delta p_{entry})_c$, such distortions will take place at a value $\dot{\gamma}_A > \dot{\gamma}_{A,j}$, i.e. after the jump. Since the length of the lower plateau region of the total pressure (p) vs $\dot{\gamma}_A$ curve (*Figure 12*) is found to increase with capillary length[6], the magnitude of the 'jump' in flow rate, $\dot{\gamma}_{A,j}-\dot{\gamma}_{A,c}$, will be enhanced accordingly. As a consequence, for a sufficiently short capillary, the 'jump' in throughput at constant pressure conditions may even take place *prior* to the onset of gross distortions, whilst for a sufficiently long capillary such distortions will commence at transient conditions.

To illustrate the significance of this 'capillary length' effect, consider the constant stress experiments of *Figure 8*, which were carried out using a standard capillary die having $L/D = 14/2$, i.e. for a capillary that is longer than the one in *Figure 12* ($L/D = 8/2$). In *Figure 8* gross melt fracture effects were found to set in transiently along the jump. The constant rate experiment of *Figure 6* (standard die) revealed that such distortions first commenced at $\dot{\gamma}_A \approx 50\,s^{-1}$, with the corresponding entry losses amounting $\Delta p_{entry} \approx 5\,MPa$, as obtained from applying the Bagley analysis[6]. This p value, arrived at from the fixed rate experiment, can be considered to be the criterion for the occurrence of gross shape distortions for the particular die geometry used, hence $(\Delta p_{entry})_c \approx 5\,MPa$. For the shorter $L/D = 8/2$ capillary (with similar entry geometry) *Figure 12* shows thatthis criterion would be attained at a value $p > p_c$ ($p_c \approx 4.25\,MPa$, i.e. at a p value outside the scale of *Figure 12*). It follows that for the case of the shorter capillary in *Figure 12* the jump would take place before gross distortions set in at higher rates (i.e. $\dot{\gamma}_A > \dot{\gamma}_{A,j}$). This would mean that the use of short capillary dies is beneficial for the control of this type of irregularity when operating under constant pressure conditions. Support for this contention has to be provided by experiment.